JMSR 1(1) (2025)

Journal of Material Science and Radiation

https://journals.balaipublikasi.id/jmsr

Effect of SnO_2 Addition on YBCO Superconducting Properties through Thermal Treatment Method

Aliah Nursyahirah Kamarudin[1], Tan Kar Yeow[1], Mohd Mustafa Awang Kechik[1*], Chen Soo Kien[1], Lim Kean Pah[1], Muhammad Kashfi Shabdin[1], Nurhidayah Mohd Hapipi[1], Muhammad Khalis Abdul Karim[1], Aris Doyan[2], Yap Siew Hong[1], Abdul Halim Shaari[1]

[1] Superconductor & Thin Films Laboratory, Department of Physics, Faculty of Science, Universiti Putra Malaysia, Selangor, Malaysia
[2] Physics Education Program, FKIP, University of Mataram, Mataram, Lombok, West Nusatenggara, Indonesia.

Received: February 13, 2025
Revised: March 29, 2025
Accepted: April 25, 2025
Published: April 30, 2025

Corresponding Author:
Mohd Mustafa Awang Kechik
mmak@upm.edu.my

Abstract: In this study, $YBa_2Cu_3O_{7-\delta}$ (YBCO) superconductors were synthesized using a thermal treatment method with the addition of 1.0 wt. % SnO_2. The synthesis of YBCO employed nitrate-based precursors and polyvinylpyrrolidone (PVP) as a capping agent to enhance homogeneity during the synthesis process. All samples were characterized using thermogravimetric analysis (TGA), X-ray diffraction (XRD), Scanning electron microscopy (SEM) and Four-point probe (4PP). TGA results of the pure YBCO sample confirmed the complete transformation of nitrate-based precursors into oxide forms prior to the formation of the YBCO phase. XRD pattern revealed that Y123 as a major phase and Y124 as a minor phase in all samples with orthorhombic crystal structure were preserved. However, the peak intensity of the Y123 was pronounced with the addition of the SnO2 sample, suggesting the enhancement phase formation due to the presence of SnO_2. The electrical resistivity measures revealed a sharp superconducting transition in all samples. However, the reduction in superconducting transition temperatures for the SnO_2 addition were observed where the $T_{c\text{-onset}}$ decreased from 91.70 K to 89.25 K for the YBCO and YBCO + 1.0 wt.% of SnO_2, respectively. This also exhibited the broadening of transition width, ΔT_c indicating the suppression of superconducting properties with SnO_2 inclusion. SEM analysis showed notable differences in microstructure. The pure YBCO sample exhibited a larger average grain size of 1.32 µm, while the YBCO + 1.0 wt. % SnO_2 sample formed small and rounded grains with smoother edges, potentially impacting intergranular connectivity and charge transport. Therefore, the addition of 1.0 wt. % SnO_2 to YBCO enhanced the formation of the Y123 phase but adversely affected the superconducting transition temperature and microstructural features. These findings highlight the dual role of SnO_2 in promoting phase purity while modifying grain morphology and electrical performance, offering insight into the optimization of dopants in high-temperature superconductors.

Keywords: Microstructural; SnO_2; Superconducting; Thermal treatment; YBCO.

Introduction

High-temperature superconductors (HTS) have gained significant attention due to their ability to exhibit superconductivity at temperatures above the boiling point of liquid nitrogen (77 K). Among the various HTS materials, $YBa_2Cu_3O_{7-\delta}$ (YBCO) is one of the most studied and widely used due to its relatively high critical temperature (T_c), good mechanical strength, and promising applications in power transmission, magnetic levitation and superconducting magnets (Paranthaman & Izumi, 2004; Sheahen, 1994; Yao & Ma, 2021). However, the performance of YBCO is strongly influenced by its microstructure, phase purity, and the

How to Cite:
Kamarudin, A. N., Yeow, T. K., Kechik, M. M. A., Kien, C. S., Pah, L. K., Shabdin, M. K., … Shaari, A. H. (2025). Effect of SnO2 Addition on YBCO Superconducting Properties through Thermal Treatment Method. *Journal of Material Science and Radiation*, *1*(1), 15–20. Retrieved from https://journals.balaipublikasi.id/index.php/jmsr/article/view/361

presence of flux pinning centers (Wu et al., 1987). To enhance these properties, various synthesis techniques such as co-precipitation, sol-gel, solid-state reaction, thermal decomposition, and thermal treatment have been employed (Abdullah et al., 2023; Dadras & Gharehgazloo, 2016; Kamarudin et al., 2022; Metin & Tepe, 2017). However, the thermal treatment method offers a straightforward and cost-effective approach for tailoring the superconducting characteristics through controlled heat treatment and phase formation (Dihom et al., 2019).

Despite its promising features, YBCO superconducting performance consists of a critical limitation which is its inability to sustain high magnetic flux in the mixed state, primarily due to its relatively low critical current density (J_c) (Hor et al., 1987; Kechik et al., 2009). This limitation prevents its superconducting performance in practical applications that require stability in strong magnetic fields. Thus, enhancing the J_c requires the production of high-quality YBCO materials with superior microstructural features, particularly strong grain connectivity and effective flux pinning sites (Kamarudin et al., 2025). One of the potential strategies to overcome this challenge is by introducing secondary phases or dopants, such as tin dioxide (SnO_2), which can act as artificial pinning centers (Kamarudin et al., 2022; Mohamed et al., 2024; Yap et al., 2024; Yusuf et al., 2019). Therefore, the thermal treatment method is chosen as the primary synthesis method due to its capability to produce dense and homogenous materials with controlled grain growth and phase formation.

Furthermore, in this study, the synthesis of pure YBCO and YBCO added with 1.0 wt. % of SnO_2 were conducted via the thermal treatment method. The primary objectives in this study are to investigate the effects of SnO_2 addition on the microstructure, phase formation, and crystal structure through comprehensive characterization techniques, particularly in enhancing its flux pinning capability and critical current density, thereby addressing its current limitations for high-field applications. It was found that the addition of SnO_2 in YBCO influenced the superconducting properties of the YBCO superconductors, which will be discussed in detail in this study.

Method

Pure YBCO and YBCO + 1.0 wt. % SnO_2 samples was carried out through a systematic using a thermal treatment method (Dihom et al., 2017). Initially, high-purity precursor powders of metal nitrate based, $Y(NO_3)_3.6H_2O$, $Ba(NO_3)_2$, $Cu(NO_3)_2.2.5H_2O$ from Alfa Aesar were accurately weighed according to the desired stoichiometric ratios of 1:2:3 and thoroughly mixed to achieve homogeneity. The 2 % of polyvinyl pyrrolidone, PVP was added as a capping agent to minimize the agglomeration of particles (Zahari et al., 2017).

The mixed solution was stirred at 80 °C with 850 rpm for 2 h. Then, the mixed solution undergoes the drying process in an oven for 24 h at 110 °C before undergoing the calcination process for 4 h, holding a temperature of 600 °C in a box furnace. The pre-calcined powder obtained was ground and calcined at 910 °C for 24 h of holding temperature with intermediate grinding. Next, 1.0 wt. % of SnO_2 was added in the YBCO powder before undergoing the pelletisation of 13 mm diameter of 5 mm thickness. Finally, the pellets were sintered at 980 °C for 24 h before slowly cooled to room temperature. Then, the YBCO sample undergoes XRD analysis to study the phase formation by using PW 3040/60 MPD X'Pert Pro Panalytical Philps DY 1861 X-ray diffractometer with CuKα radiation source (λ=1.5406Å) operated at 40 mA and 40 kV in angle 2θ range 20° to 80° with a scanning step size of 0.03°. To study the surface morphology of the YBCO with SnO_2 additions, SEM-LEO 1455 VPSEM equipped with energy dispersive X-ray spectrometer (EDX) was used. Four-point probe measurement was used to estimate the $T_{c\text{-onset}}$, $T_{c\text{-offset}}$ and ΔT_c.

Results and Discussion

Figure 1 presents the TGA curve of the pure YBCO superconductor sample, revealing a total mass loss of approximately 70%. The initial mass loss of about 7.8% occurred between 50 °C and 170 °C, attributed to the evaporation of water (Azeez, 2016; Melnikov et al., 2013). Also, it is notable observed the weight reduction, approximately 11.0%, took place between 200 °C and 300 °C due to the formation of nitric acid (HNO_3) and copper hydroxy nitrate, $Cu_2(OH)_3.NO_3$ (Ashok et al., 2015). Subsequently, $Cu_2(OH)_3.NO_3$ decomposed to CuO, contributing to a 13% mass loss within the range of 212 °C to 279 °C (Bardwell et al., 2015). The third significant decomposition event, occurring between 279 °C and 400 °C, corresponds to the breakdown of yttrium nitrate hexahydrate, $Y(NO_3)_3.6H_2O$, releasing H_2O and N_2O_5 gases. The polymer capping agent, PVP, decomposed between 400 °C and 490 °C (Azeez, 2016). A smaller mass reduction of 2.5% was observed from 550 °C to 588.5 °C, associated with the conversion of yttrium oxynitrate ($YONO_3$) into yttrium oxide (Y_2O_3). A broad and pronounced mass loss curve was observed between 650 °C and 925 °C, corresponding to the decomposition of barium nitrate into barium oxide (BaO), accompanied by the release of nitric oxide (NO) and oxygen (O_2) gases. Beyond 925 °C, the formation of

the Y123 phase occurs through the reaction of the metal oxides.

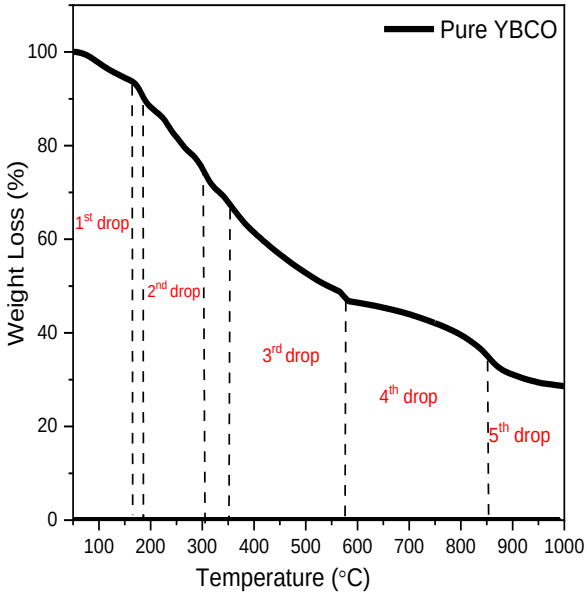

Figure 1. TGA curve analysis of pure YBCO powder. The change of the drop rate was due to the decomposition of the corresponding compound at that temperature.

For XRD analysis, Figure 2 presents the XRD pattern of pure YBCO and YBCO + 1.0 wt.% SnO_2 samples. The XRD data analysis was identified by the X'Pert Highscore Plus software with Rietveld refinement and ICSD database. It was observed that the Y123 phase was predominantly indexed as a major phase with an orthorhombic structure with the P*mmm* space group. The Y123 peaks were indexed with the reference of ICSD 98-002-7231, ICSD 98-002-9639 for Y124 and ICSD 98-000-0514 for $BaCuO_2$. Anyhow, the Y124 phase and $BaCuO_2$ phase have been detected as minor phases in all samples. These results showed that to obtain the pure Y123, thermal treatment method was an ideal method. This is because the high purity of Y123 could be obtained throughout this study by using the thermal treatment method. From the overall view of the XRD result, the peaks showed almost similar although the SnO_2 was added, but they have a slight shift of their positions. This showed that the lattice parameter of Y123 had slightly changed with added SnO_2.

It concludes that the addition of SnO_2 to pure YBCO has no significant effect on the structure and symmetry of the composites. The intensity of the peak of (103) for the sample with the addition of 1.0 wt. % of SnO_2 was lower than that of pure samples. It is agreed and supported by the reduction of intensity when the sample was added with other materials and increasing concentration of addition (Khalid et al., 2018). From Table 1, it was observed the peak intensity of the Y123 phase increased from 86.60 % to 99.80 %, indicating that it can enhance the purity of the Y123 with 1.0 wt.% SnO_2 addition. For the pure YBCO sample, the values were *a* = 3.832 Å, *b* = 3.883 Å, and *c* = 11.671 Å.

Upon the addition of SnO_2, the parameters changed of *an* increased to 3.849 Å, *c* to 11.729 Å, while *b* slightly decreased to 3.874 Å. This addition suggests that SnO_2 alters the YBCO lattice, with *a* and *c* increasing and *b* decreasing, consistent with reduced oxygen content (Howe, 2014). Also, it was found that a lower orthorhombicity factor reflects decreased oxygen content and hole concentration, which in reduces the $T_{c\text{-}onset}$ due to diminished copper chain contributions (Alecu, 2004). Higher orthorhombicity in pure YBCO indicates better. Even though the lattice parameters were slightly changed, the Y123 phases were still preserved and remained as a major phase in the YBCO sample.

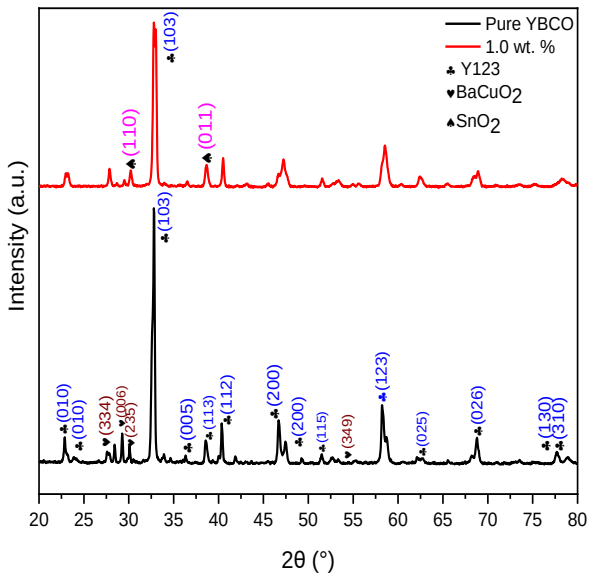

Figure 2. XRD analysis pattern of YBCO sample and YBCO + SnO_2 1.0 wt. %.

Table 1. The lattice parameters, unit cell volume and orthorhombicity factor of samples

Samples, SnO_2 (wt. %)	Lattice parameter			Phase Intensity			Unit cell volume (Å^3)	Orthorho mbi-city
	a (Å)	*b* (Å)	*c* (Å)	Y123	$BaCuO_2$	Y124		
0.0	3.832 ± 0.0003	3.883 ± 0.0003	11.671 ± 0.0011	86.60	13.40	-	173.660	0.0066
1.0	3.849 ± 0.0005	3.874 ± 0.0005	11.729 ± 0.0017	99.80	-	0.28	174.891	0.0032

The temperature-dependent electrical resistance was measured using the four-point probe technique. Figure 3 shows the normalized resistance (R_T/R_{300}) versus temperature for both the pure YBCO sample and YBCO + 1.0 wt. % of SnO_2. From the curves, all samples exhibited metallic behaviour at the normal state followed by a sharp superconducting drop to zero and the superconducting transition temperatures, Tc-onset and Tc-zero, were determined. A sharp and single-step transition was observed in both samples suggesting strong grain connectivity and the dominance of the Y123 superconducting phase (Pathak et al., 2001). The SnO_2 added with YBCO sample displayed a lower $T_{c\text{-onset}}$ compared to the pure YBCO, which correlates with its reduced orthorhombicity factor. This decrease in orthorhombicity is associated with reduced oxygen content and lower hole carrier concentration, leading to a lower $T_{c\text{-onset}}$ (Orlova & Laval, 2017). Dihom et al. (2017) also reported that higher orthorhombicity factors in YBCO are linked to higher T_c values. Additionally, the narrow superconducting transition width, ΔT_c indicates that the Y123 phase is predominant, with minor presence of secondary phases. The small differences observed in these data and this may be due to an electronic problem in the experiment (Jasim et al., 2016).

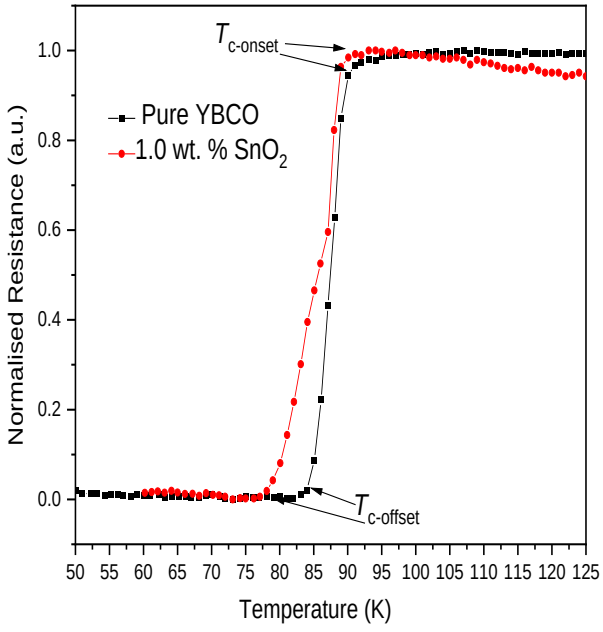

Figure 3. Graph of normalized resistance against the temperature.

To further understand the influence of SnO_2 addition in the microstructural morphology of YBCO samples, an SEM analysis was performed, as presented in Figure 4. At a lower magnification of 1500, it was observed that pure YBCO samples had a rounder shape, closely packed to each other and a slight needle shape grain that was oriented towards the same direction of one side. These distributions can be correlated with the high $T_{c\text{-onset}}$ value obtained. However, the random arrangement of the grains was observed in sample YBCO + 1.0 wt. % SnO_2, thus forming the agglomeration of the grains. At a higher magnification of 5000, the average grain size of the sample was determined using Image-*J* software by selecting 100 grains randomly to calculate the average grain size. In Table 1, it was observed that the average grain size for pure YBCO and YBCO + 1.0 wt. % SnO_2 was 1.24 µm and 1.32 µm, respectively. The slight increase in the grain sizes of YBCO sample may be due to the incorporation of SnO_2 in the YBCO thus led to the formation of a new phase within the material. Although the grains were uniformly distributed, they exhibited poor connectivity, resulting in inhomogeneities that introduced non-superconducting regions within the YBCO matrix. This disrupted the connectivity at the grain boundaries and prevented the flow of supercurrent across them. Consequently, the appearance of white regions was observed, which may be attributed to the presence of the added SnO_2. This also can be correlated with the reduction of $T_{c\text{-onset}}$ in YBCO + 1.0 wt. % SnO_2 sample which degrading the superconducting properties of YBCO samples.

Table 2. $T_{c\text{-onset}}$, $T_{c\text{-offset}}$, ΔT_c and average grain sizes of YBCO and YBCO + 1.0 wt. % SnO_2 samples.

Weight Percentage of SnO_2 (wt. %)	$T_{c\text{-onset}}$ (K)	$T_{c\text{-offset}}$ (K)	ΔT_c (K)	Average grain size (µm)
0.0	91.70	83.20	8.50	1.24
1.0	89.25	76.04	13.21	1.32

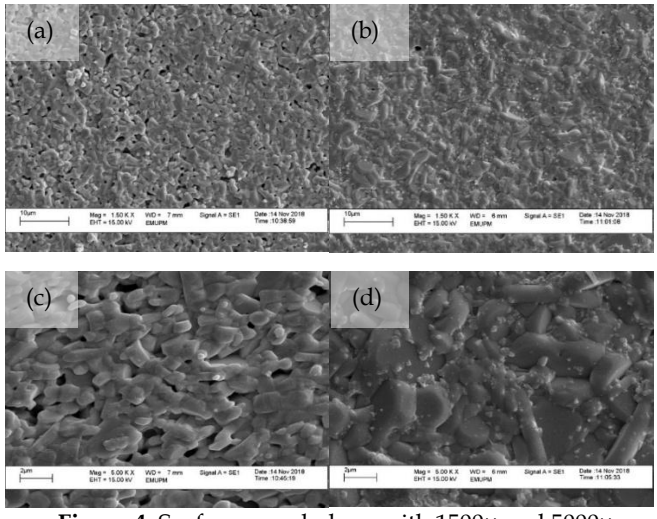

Figure 4. Surface morphology with 1500× and 5000× magnification of pure YBCO sample and YBCO added with 1.0 wt. % SnO_2. The images showed the result of of (a), (c) pure YBCO sample and (b), (d) YBCO + 1.0 wt. % SnO_2.

Conclusion

YBCO superconductors with SnO_2 addition were successfully synthesized via thermal treatment and sintering without oxygen flow. From XRD analysis, the incorporation of 1.0 wt. % SnO_2 enhanced the Y123 phase purity and promoted oriented grain growth, as reported in XRD and SEM analysis. Despite a reduction in orthorhombicity and superconducting transition temperature, $T_{c\text{-onset}}$ of YBCO bulk samples due to the weakened grain connectivity and increased lattice strain, the formation of larger, rounder grains with reduced porosity were observed in YBCO + 1.0 wt % SnO_2 microstructural features. In conclusion, these findings demonstrate that controlled SnO_2 addition can optimise the phase formation and microstructure, thus offering enhanced phase purity and superconducting performance of YBCO bulk samples.

Acknowledgments
This research was funded by the Ministry of Higher Education Malaysia through the Fundamental Research Grant Scheme (FRGS) under project number FRGS 1/2017/STG02/UPM/02/4, grant number FRGS 5546036.

Author Contributions
Conceptualization, M.M.A.K, T.K.Y. and A.N.K.; methodology, T.K.Y.; software, A.N.K.; validation, M.M.A.K., C.S.K. L.K.P, A.D. and A.H.S.; formal analysis, T.K.Y. and M.M.A.K.; investigation, T.K.Y and A.N.K.; resources, M.M.A.K.; data curation, T.K.Y. and A.N.K.; writing—original draft preparation, T.K.Y. and A.N.K..; writing—review and editing, A.N.K., M.M.A.K., A.D. and Y.S.H.; visualization, M.K.A.K, Y.S.H. and M.K.S.; supervision, C.S.K., L.K.P. and A.H.S.; project administration, M.M.A.K.; funding acquisition, M.M.A.K. All authors have read and agreed to the published version of the manuscript.

Funding
The authors declare no external finding.

Conflicts of Interest
The authors declare no conflict of interest.

References

Abdullah, S. N., Kechik, M. M. A., Kamarudin, A. N., Talib, Z. A., Baqiah, H., Kien, C. S., Pah, L. K., Abdul Karim, M. K., Shabdin, M. K., Shaari, A. H., Hashim, A., Suhaimi, N. E., & Miryala, M. (2023). Microstructure and Superconducting Properties of Bi-2223 Synthesized via Co-Precipitation Method: Effects of Graphene Nanoparticle Addition. *Nanomaterials*, *13*(15). https://doi.org/10.3390/nano13152197

Alecu, G. (2004). Crystal Structures of Some High-Temperature Superconductors. *Romanian Reports in Physiscs*, *56*(3), 404–412. Retrieved from https://shorturl.asia/5Vjbq

Azeez, N. (2016). Thermogravimetric Analysis on PVA/PVP Blend Under Air Atmosphere. *Engineering and Technology Journal*, *34*(13), 2433–2441. https://doi.org/10.30684/etj.34.13A.6

Bardwell, C. J., Bickley, R. I., Poulston, S., & Twigg, M. V. (2015). Thermal decomposition of bulk and supported barium nitrate. *Thermochimica Acta*, *613*(3), 94–99. https://doi.org/10.1016/j.tca.2015.05.013

Dadras, S., & Gharehgazloo, Z. (2016). Effect of Au nano-particles doping on polycrystalline YBCO high temperature superconductor. *Physica B: Physics of Condensed Matter*, *492*, 45–49. https://doi.org/10.1016/j.physb.2016.04.005

Dihom, M. M., Shaari, A. H., Baqiah, H., Al-Hada, N. M., Kean, C. S., Azis, R. S., Kechik, M. M. A., & Abd-Shukor, R. (2017). Effects of calcination temperature on microstructure and superconducting properties of Y123 ceramic prepared using thermal treatment method. *Solid State Phenomena*, *268 SSP*, 325–329. Retrieved from https://www.scientific.net/SSP.268.325

Dihom, M. M., Shaari, A. H., Baqiah, H., Al-Hada, N. M., Kien, C. S., Azis, R. S., Kechik, M. M. A., Talib, Z. A., & Abd-Shukor, R. (2017). Microstructure and superconducting properties of Ca substituted Y(Ba1−xCax)2Cu3O7−δ ceramics prepared by thermal treatment method. *Results in Physics*, *7*, 407–412. https://doi.org/10.1016/j.rinp.2016.11.067

Hor, P. H., Gao, L., Meng, R. L., Huang, Z. J., Wang, Y. Q., Forster, K., Vassilious, J., Chu, C. W., Wu, M. K., Ashburn, J. R., & Torng, C. J. (1987). High-pressure study of the new Y-Ba-Cu-O superconducting compound system. *Physical Review Journals*, *58*(9), 911–912. https://doi.org/10.1103/PhysRevLett.58.911

Howe, B. A. (2014). *Crystal Structure and Superconductivity of YBa2Cu3O 7–x*. Mankato: Minnesota State University.

Jasim, S. E., Jusoh, M. A., Hafiz, M., & Jose, R. (2016). Fabrication of Superconducting YBCO Nanoparticles by Electrospinning. *Procedia Engineering*, *148*, 243–248. https://doi.org/10.1016/j.proeng.2016.06.595

Kamarudin, A. N., Awang Kechik, M. M., Abdullah, S. N., Baqiah, H., Chen, S. K., Abdul Karim, M. K., Ramli, A., Lim, K. P., Shaari, A. H., Miryala, M., Murakami, M., & Talib, Z. A. (2022). Effect of Graphene Nanoparticles Addition on Superconductivity of YBa2Cu3O7~δ Synthesized via the Thermal Treatment Method. *Coatings*, *12*(1), 91. https://doi.org/10.3390/coatings12010091

Kamarudin, A. N., Muralidhar, M., Kechik, M. M. A., Chen, S. K., Lim, K. P., Harun, M. H., Shabdin, M. K., Karim, M. K. A., & Shaari, A. H. (2025). Elucidating of Er211 performance in (Y,Er)Ba2Cu3Oy single-grain bulk superconductors by infiltration growth process. *Physica B: Condensed Matter*, *706*, 417152. https://doi.org/10.1016/j.physb.2025.417152

Kechik, M. M. A., Mikheenko, P., Sarkar, A., Dang, V. S., Hari Babu, N., Cardwell, D. A., Abell, J. S., & Crisan, A. (2009). Artificial pinning centres in YBa 2 Cu 3 O 7−δ thin films by Gd 2 Ba 4 CuWO y nanophase inclusions. *Superconductor Science and Technology*, *22*(3), 034020. https://doi.org/10.1088/0953-2048/22/3/034020

Khalid, N. A., Kechik, M. M. A., Baharuddin, N. A., Kien, C. S., Baqiah, H., Yusuf, N. N. M., Shaari, A. H., Hashim, A., & Talib, Z. A. (2018). Impact of carbon nanotubes addition on transport and superconducting properties of YBa2Cu3O7−δ ceramics. *Ceramics International*, *44*(8), 9568–9573. https://doi.org/10.1016/j.ceramint.2018.02.178

Melnikov, P., Nascimento, V. A., Consolo, L. Z. Z., & Silva, A. F. (2013). Mechanism of thermal decomposition of yttrium nitrate hexahydrate, Y(NO3)3·6H2O and modeling of intermediate oxynitrates. *Journal of Thermal Analysis and Calorimetry*, *111*(1), 115–119. https://doi.org/10.1007/s10973-012-2236-3

Metin, T., & Tepe, M. (2017). The Effect of Ag Doping on the Superconducting Properties of Y3Ba5Cu8−xAgxO18−δ Ceramics. *Journal of Superconductivity and Novel Magnetism*, *30*(4), 1083–1087. https://doi.org/10.1007/s10948-016-3768-8

Mohamed, A. R. A., Awang Kechik, M. M., Chen, S. K., Lim, K. P., Baqiah, H., Shariff, K. K. M., Yap, S. H., Hoo, K. P., Shaari, A. H., Humaidi, S., & Muralidhar, M. (2024). Enhancing superconducting properties of YBa2Cu3O7- δ through Nd2O3 addition prepared using modified thermal decomposition method. *Applied Physics A: Materials Science and Processing*, *130*(12), 897. https://doi.org/10.1557/proc-275-49

Orlova, T. S., & Laval, J. Y. (2017). Microstructure and superconducting properties of the DyBaCuO ceramic doped with Na2CO3, NaCl, and KClO3. *Physics of the Solid State*, *49*(11), 2058–2064. https://doi.org/10.1134/S1063783407110078

Paranthaman, M. P., & Izumi, T. (2004). High-performance YBCO-coated superconductor wires. *MRS Bulletin*, *29*(8), 533–537. https://doi.org/10.1557/mrs2004.159

Pathak, L. C., Mishra, S. K., Das, S. K., Bhattacharya, D., & Chopra, K. L. (2001). Effect of sintering atmosphere on the weak-link behaviour of YBCO superconductors. *Physica C: Superconductivity and Its Applications*, *351*(3), 295–300. https://doi.org/10.1016/S0921-4534(00)01628-2

Sheahen, T. P. (1994). *Introduction to High temperature superconductivity*. Springer Science & Business Media.

Wu, M. K., Ashburn, J. R., Torng, C. J., Hor, P. H., Meng, R. L., Gao, L., Huang, Z. J., Wang, Y. Q., & Chu, C. W. (1987). Superconductivity at 93 K in a new mixed-phase Yb-Ba-Cu-O compound system at ambient pressure. *Physical Review Letters*, *58*(9), 908–910. https://doi.org/10.1103/PhysRevLett.58.908

Yao, C., & Ma, Y. (2021). Superconducting materials: Challenges and opportunities for large-scale applications. *IScience*, *24*(6), 102541. https://doi.org/10.1016/j.isci.2021.102541

Yap, S. H., Kechik, M. M. A., Shariff, K. K. M., Baqiah, H., Chen, S. K., Lim, K. P., Shabdin, M. K., Zaid, M. H. M., Yaakob, Y., Karim, M. K. A., Humaidi, S., Shaari, A. H., & Miryala, M. (2024). Fluctuation induces conductivity and microstructural studies in Y-123: Effect of CaO inclusion. *Journal of Alloys and Compounds*, *1005*(August), 175955. https://doi.org/10.1016/j.jallcom.2024.175955

Yusuf, N. N. M., Kechik, M. M. A., Baqiah, H., Kien, C. S., Pah, L. K., Shaari, A. H., Jusoh, W. N. W. W., Sukor, S. I. A., Dihom, M. M., Talib, Z. A., & Abd-Shukor, R. (2019). Structural and superconducting properties of thermal treatment-synthesised bulk YBa2Cu3O7-δ superconductor: Effect of addition of SnO2 nanoparticles. *Materials*, *12*(1), 6–15. https://doi.org/10.3390/ma12010092

Zahari, R. M., Shaari, A. H., Abbas, Z., Baqiah, H., Chen, S. K., Lim, K. P., & Kechik, M. M. A. (2017). Simple preparation and characterization of bismuth ferrites nanoparticles by thermal treatment method. *Journal of Materials Science: Materials in Electronics*, *28*(23), 17932–17938. https://doi.org/10.1007/s10854-017-7735-3